JOINT EUROPEAN TORUS

JET–P(91)17

N.J. Lopes Cardozo, A.C.C. Sips
and JET Team

Sawtooth Heat Pulse Propagation in Tokamaks

Sawtooth Heat Pulse Propagation in Tokamaks

N.J. Lopes Cardozo[1], A.C.C. Sips
and JET Team*

JET-Joint Undertaking, Culham Science Centre, OX14 3DB, Abingdon, UK

[1]FOM Instituut voor Plasmafysica "Rijnhuizen", Nieuweigen, the Netherlands
** See Appendix 1*

Preprint of Paper to be submitted for publication in
Plasma Physics and Controlled Fusion

SAWTOOTH HEAT PULSE PROPAGATION IN TOKAMAKS

N.J. Lopes Cardozo[1] and A.C.C. Sips

JET Joint Undertaking, Abingdon, Oxon, OX14 3AE, United Kingdom

[1]: FOM Instituut voor Plasmafysica "Rijnhuizen", Nieuwegein, the Netherlands

Abstract

Standard analysis treats the sawtooth induced heat pulse as a diffusive phenomenon by linearising the diffusion equation around the unperturbed state of the plasma. This implies that the heat pulse is governed by the *incremental* thermal diffusivity. This approach has been criticized by Fredrickson et al [1], who claim that turbulence associated with the sawtooth collapse affects the propagation of the heat pulse. It is shown that due to a fundamental misconception their modelling with a time–dependent diffusivity (the 'ballistic' heat pulse) is incorrect and leads to invalid conclusions. We demonstrate that the measurements impose a temporary change of the effective thermal diffusivity during the heat pulse which is similar to the implicit time behaviour imposed by the linearised treatment.

Introduction

The physics of transport of heat and particles in Tokamak plasmas has been recognized as a key subject for research for some years. It has direct relevance for the development of a Tokamak type fusion reactor: the size of such a machine is largely determined by the lowest achievable thermal diffusivity of the plasma, whereas the ash–removal in a burning plasma relies on sufficiently rapid particle diffusion.

There are two different approaches to transport studies in magnetically confined thermonuclear plasmas: static power balance analysis and perturbative transport studies. In the power balance method fluxes and gradients are evaluated. For example, the effective thermal diffusivity for the electrons is determined as the ratio of the electron heat flux (q_e) and the product of the electron density (n_e) and temperature gradient (∇T): $\chi^{eff} = q/(n\nabla T)$ (the subscript e has been omitted, and will be in the remainder of the paper, for clarity of notation). Perturbative techniques, on the other hand, employ a perturbation of a steady plasma state. The temperature is measured as a function of space and time, and from this behaviour the diffusivity can be determined [2]. In particular, the adiabatic perturbation of the central part of the electron temperature profile induced by the sawtooth instability is widely used. This is known as sawtooth heat pulse propagation. The method was first proposed by Callen and Jahns [3] and has since been applied to many Tokamaks.

The standard approach treats the heat pulse as a diffusive process. Tubbing et al [4] have shown, by linearising the transport equations, that the propagation of the heat pulse is governed by the incremental diffusivity $\chi^{inc} = \partial(q)/\partial(n\nabla T)$ (see Fig. 1). χ^{inc} often exceeds χ^{eff} by a factor between 1 and 5. This difference can be explained by a non–linear dependence of the heat flux on the temperature gradient. The values of χ^{inc} from heat pulse analysis are corroborated by other perturbative methods, such as modulated power deposition and pellet injection [5,6,7].

Recently, the standard treatment has been criticized by Fredrickson et al [1], who claim that diffusion alone fails to describe TFTR heat pulses. In this paper we show that a fundamental error lies at the basis of this conclusion. In [1] the diffusive modelling is started during the sawtooth collapse rather than after, so that the analysis incorrectly includes part of the MHD instability.

In this paper we first re–analyse the TFTR data presented in [1], and show that by starting the analysis after the sawtooth collapse, diffusive modelling does give an adequate description of these measurements. This is followed by a general assessment of models with an

explicit time dependence for χ^{eff}. It is demonstrated that the model proposed in [1] does not match the TFTR measurements. We show that the experimental data put such strong constraints on a possible time dependence for χ^{eff} that the difference with the implicit time dependence imposed by linearising the transport equations becomes semantic.

Analysis of TFTR heat pulse data using linearised transport equations

Whereas in the power balance studies conduction and convection may both play a role, in the relaxation of a localised perturbation the contribution of the highest order spatial derivatives, the diffusion terms, is dominant. This is a result of the small scale lengths of the initial perturbation compared to the steady state values. Hence the relaxation of a localised perturbation of the electron temperature is to good approximation described by

$$\frac{3}{2}\frac{\partial(nT_1)}{\partial t} = \nabla\,(n\chi^{inc}\nabla T_1) \tag{1}$$

The subscript 1 denotes a perturbation with respect to a steady state (subscript 0). The diffusion is governed by the incremental diffusion coefficient χ^{inc}, defined by

$$\chi^{inc} = \chi^{eff} + (\frac{\partial\chi^{eff}}{\partial\nabla T})\nabla T_0 = \frac{\partial q}{\partial(n\nabla T)} \tag{2}$$

The thermal diffusivity may be a function of ∇T, and it is therefore incorrect to equate χ^{inc} to χ^{eff} (see Fig 1).

The applicability of eqn (1) is confined to regions where $|\nabla T_1| / |\nabla T_0| << 1$ and where the source density is not significantly perturbed. Furthermore, the analysis cannot be expected to give meaningful results when gross MHD phenomena occur in the region in which it is applied.

For sawtooth heat pulse propagation, diffusive modelling can be applied outside the region where the temperature is perturbed during the sawtooth crash. This region is bounded by the so called mixing radius (r_{mix}). The definition of r_{mix} may vary within different theoretical models for the sawtooth instability, but experimentally the definition is quite clear as is shown from measurement of T at JET (Fig. 2). Allowing some safety margin, heat pulse analysis can be applied outside the experimentally observed mixing radius.

A numerical simulation of the heat pulse can be obtained by two different techniques: a) The measured temperature evolution just outside r_{mix} can be used as a boundary condition, while the other boundary is applied at the limiter, where the perturbed temperature is to good approximation zero. b) The heat pulse can be treated as an initial value problem, which is started after the sawtooth collapse. Simulation of JET data show that the two approaches generally yield the same value for χ^{inc} in the heat pulse region, and that for $r > r_{mix}$ the solutions of the initial value problem are nearly identical to solutions of the forced boundary problem. This result justifies the use of quick methods to determine χ^{inc} which are based on solutions of the initial value problem, such as the extended time–to–peak method developed at JET [2].

We have analysed heat pulse data from TFTR using both forced boundary and initial value methods, using the numerical codes developed at JET. These calculations are based on a linearisation of the transport equations which includes the effects of coupling between energy and particle transport [8,9]. The results are shown in Fig 3. For both methods $\chi^{inc} \approx$ 12 m^2/s in the heat pulse region. The same value is found with the extended time–to–peak method [1]. For comparison, $\chi^{eff} = 3.8$ m^2/s averaged over the heat pulse region.

Fredrickson et al. have simulated the same data with the initial value method, taking a mixing radius which is significantly smaller than that observed experimentally. No satisfactory agreement with the data is obtained. The choice of this smaller mixing radius has significant effects: 1) the amplitude of the heat pulse at $r > r_{mix}$ is an order of magnitude too low[1], and 2) at $r = 0.4$ m., just outside the experimental mixing radius, the simulated heat pulse shows a delayed peaking time compared to the measurements. Fredrickson et. al. [1] claim that their results show that the heat pulse has a ballistic contribution, but this conclusion is in error and is due to the use of an incorrect initial condition.

Time dependent diffusivity modelling

Although linearised diffusive modelling appears adequate for the heat pulse measurements of TFTR and JET, it is interesting to investigate the possibility of describing the evolution of the full electron temperature profile. In this case the linearisation around the steady state cannot be applied. Since in general $\chi^{inc} > \chi^{eff}$, solving the transport equations with fixed

[1] *This is not apparent from the figures in ref [1], because there the simulated traces have been scaled by arbitrary factors to match the measured amplitude [10].*

$\chi = \chi^{eff}$ leads to a slower propagation of the heat pulse than experimentally observed. Consequently, a temporary enhancement of χ should be introduced.

In the linearised diffusive modelling a time dependent enhancement of χ^{eff} is implicit through the functional dependence of χ^{eff} on the local temperature gradient (see Fig. 1). Fig. 4 shows the evolution of ∇T during the heat pulse; the enhancement of χ travels slightly ahead of the heat pulse. Also the deviation of χ^{eff} from the equilibrium value is proportional to the amplitude of the perturbation.

An enhancement of χ of a different origin might be caused by the sawtooth collapse itself, based on the idea that the collapse induces a temporary increase in the level of turbulence in the plasma. The diffusivity should return to its steady state value χ^{eff} with a characteristic decay time τ. A generic form of the enhancement of χ may be given by

$$\chi = \chi^{eff}\,(1 + f(r)\exp(-t/\tau)) \tag{3}$$

The response of the temperature profile to a temporary enhancement of χ can be determined by inserting the expression (3) for χ in the transport equation to obtain

$$\frac{\partial}{\partial t}(\frac{3}{2}nT) = \frac{1}{r}\frac{\partial}{\partial r}(rn\chi^{eff}\frac{\partial T}{\partial r}) + P(r) + \frac{1}{r}\frac{\partial}{\partial r}(rn\chi^{eff}f(r)\frac{\partial T}{\partial r})\exp(-t/\tau) \tag{4}$$

where $P(r)$ is the power density in the plasma. Just after the sawtooth collapse the first two terms on the r.h.s. add up to zero outside the mixing radius. Hence, $\partial T/\partial t$ is determined by $f(r)$ and the unperturbed values of n and ∇T; the T–profile adjusts itself to the new χ–profile.

Fredrickson et. al. [1] have used an explicit time dependence of χ^{eff} to model the heat pulse in TFTR. The decay time τ is taken short compared to the diffusion time and consequently the enhancement factor must be taken large to have any effect at all. It is claimed that the measurements of the heat pulse of shot 30904 at TFTR can be modelled taking the following function for $f(r)$:

$$f(r) = 150\exp(-9.6(r/a)^2), \quad \text{for } \tau = 1\text{ ms}$$

An important characteristic of this model is the initial rise of the temperature just after the sawtooth collapse outside the mixing radius. This can be calculated analytically from eqn (4) and compared with the measurements at $r = 0.40$ m and $r = 0.65$ m (see Table I).

Table I:
The calculated initial rise of the electron temperature outside the mixing radius using the data presented in [1] in expression (3) in this paper. The results are compared with the measurements [1].

Radius	r = 0.40 m	r = 0.65 m
$\frac{\partial T}{\partial t}$ (TFTR model)	600 keV/s	90 keV/s
$\frac{\partial T}{\partial t}$ (measurements)	500 keV/s	<35 keV/s

From this table it is clear the model predicts a much faster rise of the temperature at r = 0.65 m than is observed. For a more detailed comparison, Fig.5a shows the full numerical simulations using this model, as reproduced by us. A reasonable match to the data is found at r = 0.40 m, but in the centre and at r = 0.65 m the model is clearly in error.

These results are apparently in contradiction with ref [1], where good agreement between model and measurements is claimed in the heat pulse region. This agreement appears to exist only for the shape of the temperature traces. The amplitude, which in [1] has been scaled to fit the measurements, is not consistent with the experimental data. The application of scaling factors, however, is not allowed since the scaled results are no longer a solution of the transport equations. The discrepancy in the centre, in the first few milliseconds after the sawtooth collapse is also non–trivial, because it is directly related to the choice of time–constant τ. The failure of the model is clearly demonstrated in Fig 5b, where the perturbation generated by the time–dependent χ is compared with the experimental data.

It is useful to consider variations on the proposed model in order to characterise the temporal enhancement required to describe the heat pulse. First, by decreasing τ to 0.1 ms and applying a very strong enhancement of χ in the central region out to the measured mixing radius, it is possible to obtain a good fit to the measurements in the centre. However, since after a fraction of a millisecond the diffusivity has returned to its unperturbed value, the subsequent heat pulse is inevitably too slow (Fig 6).

Alternatively, the enhancement of χ can be restricted to a part of the plasma around the mixing radius, while keeping the longer time constant τ. In this case it is necessary to

start with the correct initial profile, since the enhancement of χ now cannot replace a part of the sawtooth collapse. However, as shown in Fig. 6, this still fails to reproduce the experimental data satisfactory.

Generally we find that in models featuring a single time constant for the enhancement, it is not possible to fit the heat pulse both near the mixing radius and further out. Whereas it might seem that with sufficient parameters in f(r) it should be possible to give a satisfactory simulation of the heat pulse, in fact there is not much freedom. It appears to be necessary to have a radially dependent time constant, such that the enhancement is slower further away from the mixing radius. In this way, however, we have recovered the characteristics of the implicit time dependence of χ^{eff} in the linearised diffusive modelling.

Discussion and Conclusions

We have shown that modelling using linearised transport equations is a very suitable approach for the analysis of sawtooth heat pulses. The so–called 'ballistic' contributions to the heat pulse reported in TFTR appear to be diffusive, like the heat pulse in other Tokamaks. The fact that the value for χ derived from heat pulse analysis exceeds the power balance value is due to the fact that the two are different quantities: the heat pulse evaluates the incremental diffusivity, whereas power balance yields the effective diffusivity.

An investigation of the time dependent modelling shows two things. Firstly, the results presented in [1] are incorrect and the model can not be corrected without changing it fundamentally. Secondly, from a trial–and–error procedure, we have concluded that for a time dependent model to match the data, it must have characteristics similar to the implicit time dependence of χ^{eff} in the diffusive (i.e. standard) model.

One could still maintain that the fast propagation is not due to a diffusive process but that χ is enhanced by some other process in such a way that the heat pulse looks like a diffusive relaxation. In this interpretation the heat pulse would not give meaningful information on the transport in a Tokamak plasma. However, this interpretation can hardly be maintained since other perturbative methods, not involving the sawtooth collapse, give similar values for χ^{inc}. In addition, the enhanced turbulence level does not seem to affect the sawtooth density pulse, which is much slower than the heat pulse in TFTR (as is the case in JET).

We have shown that a correct interpretation of both heat and density pulse can be obtained for measurements at JET and TEXT if coupling between the sawtooth induced

density pulse and heat pulse is included in the analysis [11,12]. In this respect it is interesting to note that in TFTR a coupling of the heat pulse and the density pulse is also present (as illustrated in Fig 3).

Acknowledgements

The authors are indebted to many people at JET, in particular Drs. Boucher, Campbell, Cordey, Costley, Keilhacker, Kramer, O'Rourke, Stott, Watkins and Wesson for their stimulating discussions on the subject. The authors are also grateful for the discussions with Dr Fredrickson from TFTR. Part of this work was performed under the EURATOM–FOM association agreement with financial support from NWO and EURATOM.

References

[1] E.D. Fredrickson et al, Phys Rev Lett. **65** (1990) 2869

[2] N.J. Lopes Cardozo et al, Plasma Physics and Controlled Fusion **32** (1990) 983

[3] J.D. Callen and G.L. Jahns, Phys Rev Lett. **38** (1977) 971

[4] B.J.D. Tubbing, N.J. Lopes Cardozo and M.J. van der Wiel, Nucl. Fusion **27** (1987) 1843

[5] D.F.H. Start et al, Nucl Fusion Suppl. **Vol 1** (1989) 593

[6] D.J. Gambier et al, Nuclear Fusion **30** (1990) 23

[7] A. Gondhalekar et al, PLasma Physics and Controlled Fusion **31** (1989) 805

[8] G.M.D. Hogeweij, J. O'Rourke and A.C.C. Sips, Plasma Physics and Controlled Fusion, **Vol 33(3)**, (1991), 189

[9] K.W. Gentle, Phys. of Fluids **31** (1988) 1105

[10] E.D. Fredrickson, private communication, March 1991

[11] J.C.M. de Haas, J. O'Rourke, A.C.C. Sips, and N.J. Lopes Cardozo, to be published in Nuclear Fusion, also JET report **JET–R(90)04**

[12] A.C.C. Sips et al, to be published in Nuclear Fusion, also JET report **JET–P(91)01**.

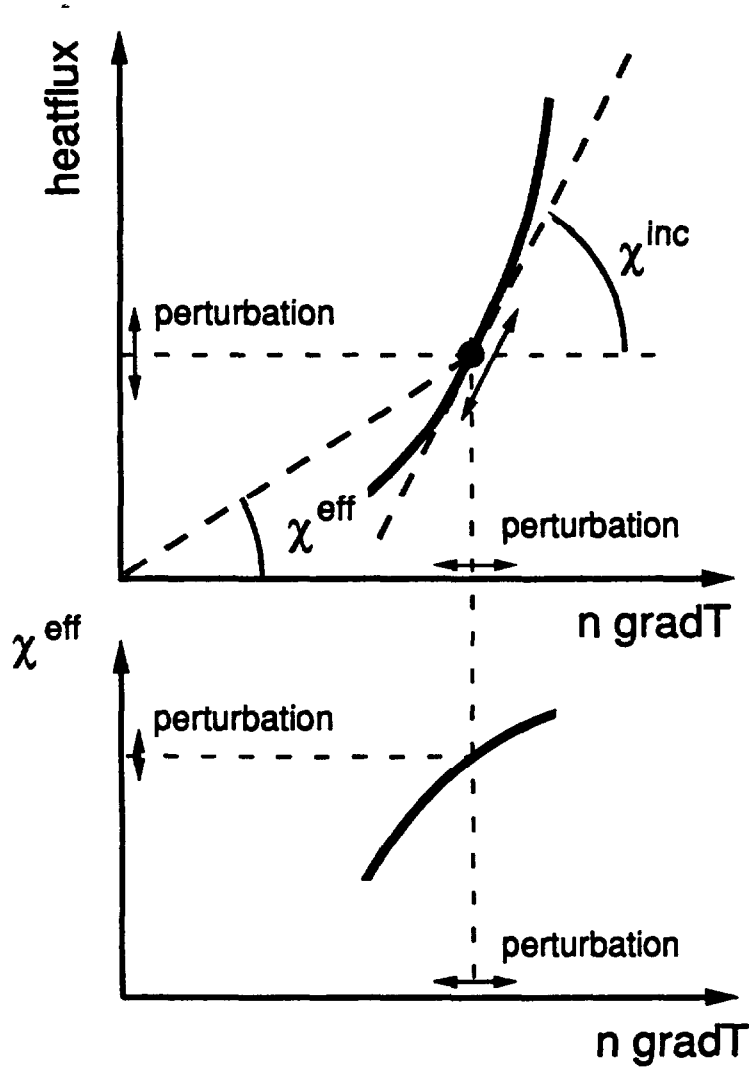

Figure 1

A power balance in a stationary plasma evaluates the heat flux and the temperature gradient to determine the effective diffusivity χ^{eff}. In perturbative experiments, flux and gradient are varied around the equilibrium value, and thus the incremental diffusivity χ^{inc} is found. Note that χ^{eff} varies along with ∇T during the perturbation.

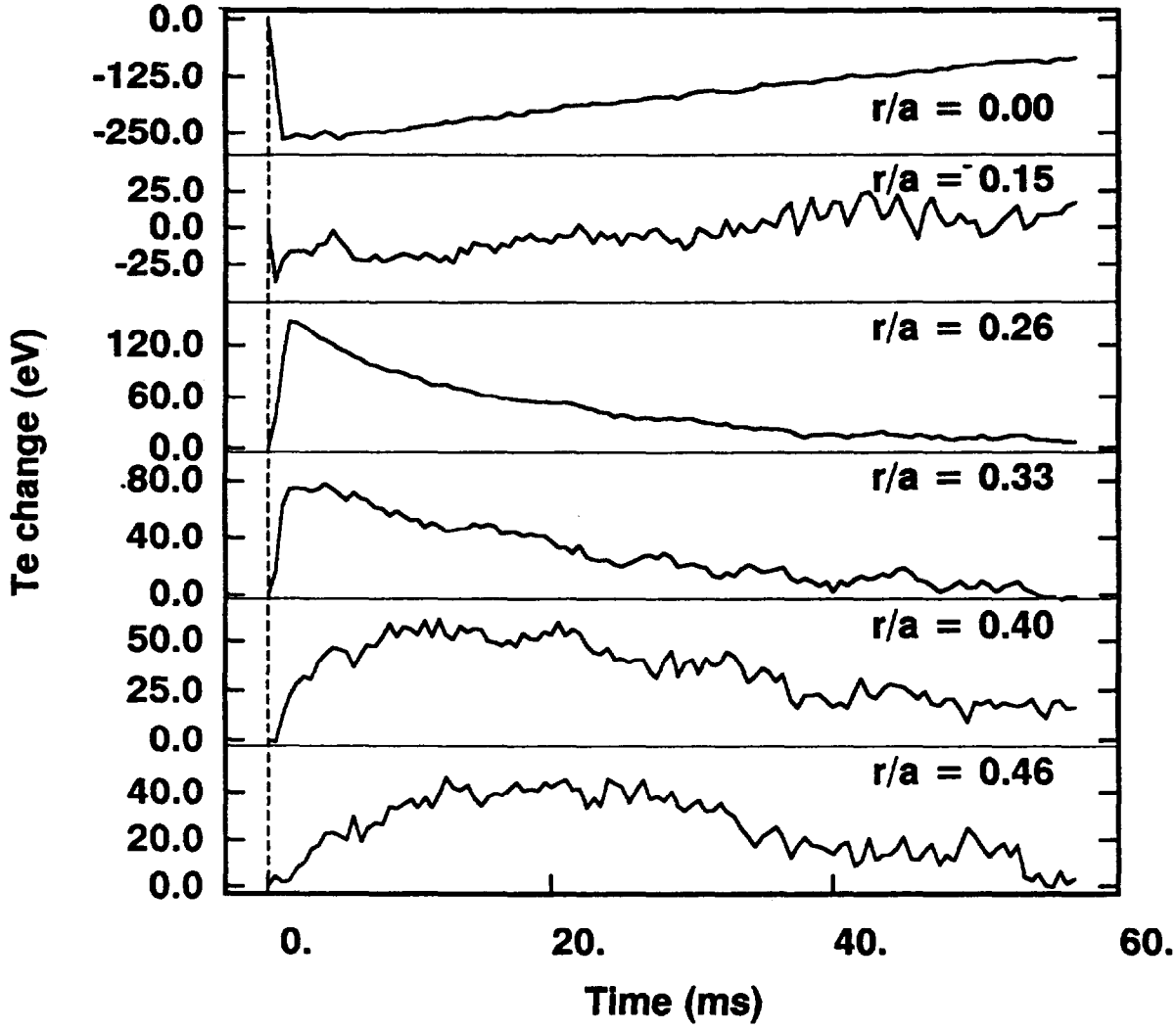

Figure 2

Measurements of the electron temperature in JET during a sawtoothing discharge, showing the different time behaviour inside and outside the mixing radius (# 19761: 3MA/3.4T).

At r/a = 0.0 the fast collapse and immediate reheating of the electron temperature is observed. The inversion radius is near r/a = 0.15 where the temperature has little response to the sawtooth collapse. The temperature variation at r/a = 0.26 is typical for the region between the inversion radius and the mixing radius, the initial rise is fast and the perturbation decays quickly. The ECE channels outside the mixing radius are: r/a = 0.33 (just outside r_{mix}, the rise time is fast and the decay is slow), r/a = 0.40 and r/a = 0.46 since they show a delayed peaking of the temperature (heat pulse).

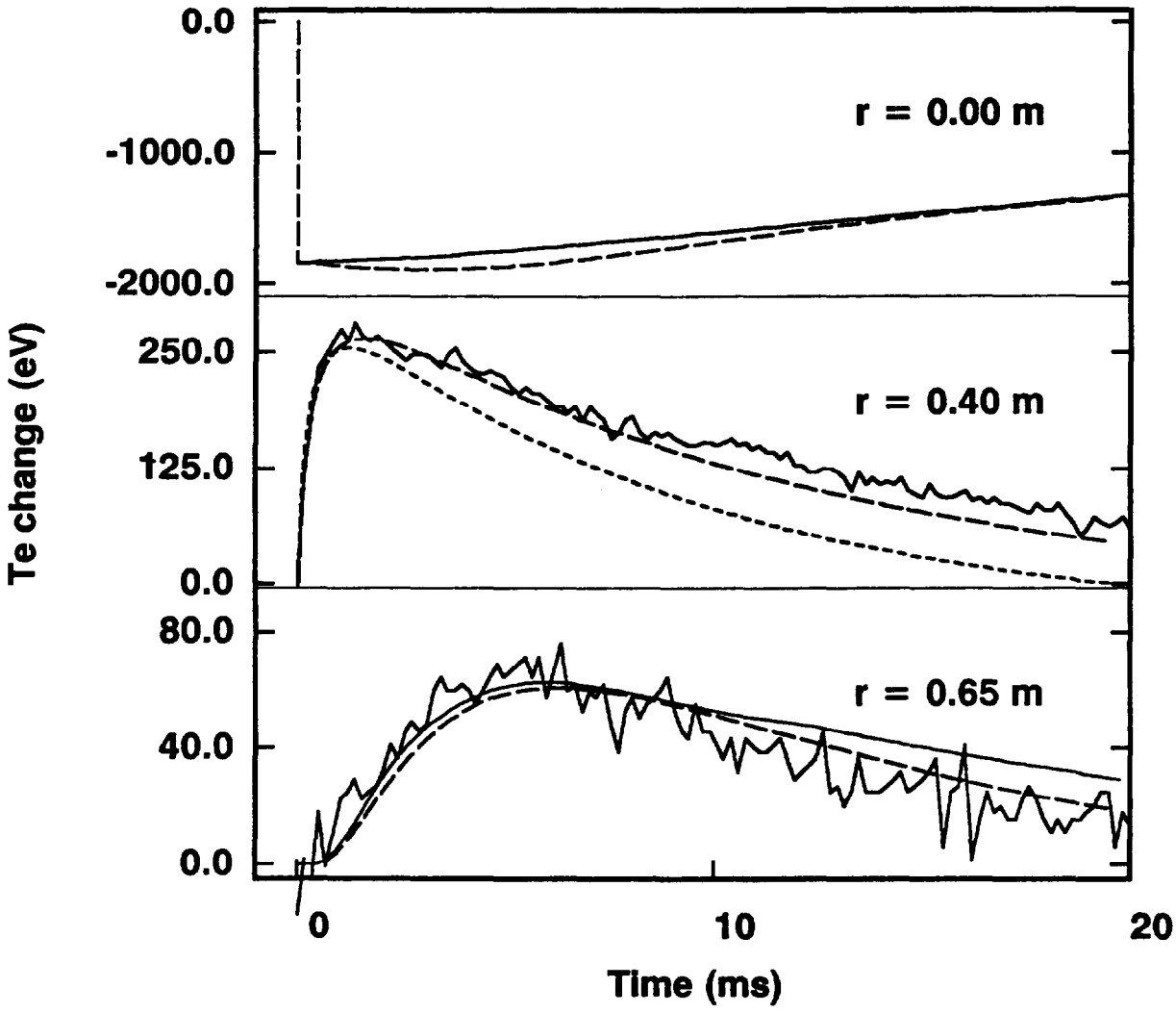

Figure 3

Heat pulse measurements from TFTR (solid lines, taken from ref[1]), re–analysed with the forced boundary (measurements at r = 0.40 m applied as boundary condition, simulated is the response at r = 0.65 m, thin full line) and initial value method (dashed line), using linearised coupled transport equations. Both methods provide a satisfactory description of the data. The effects of the cross–coupling with the density pulse improves the fit in the tail of the heat pulse at r = 0.40 m (dotted line).

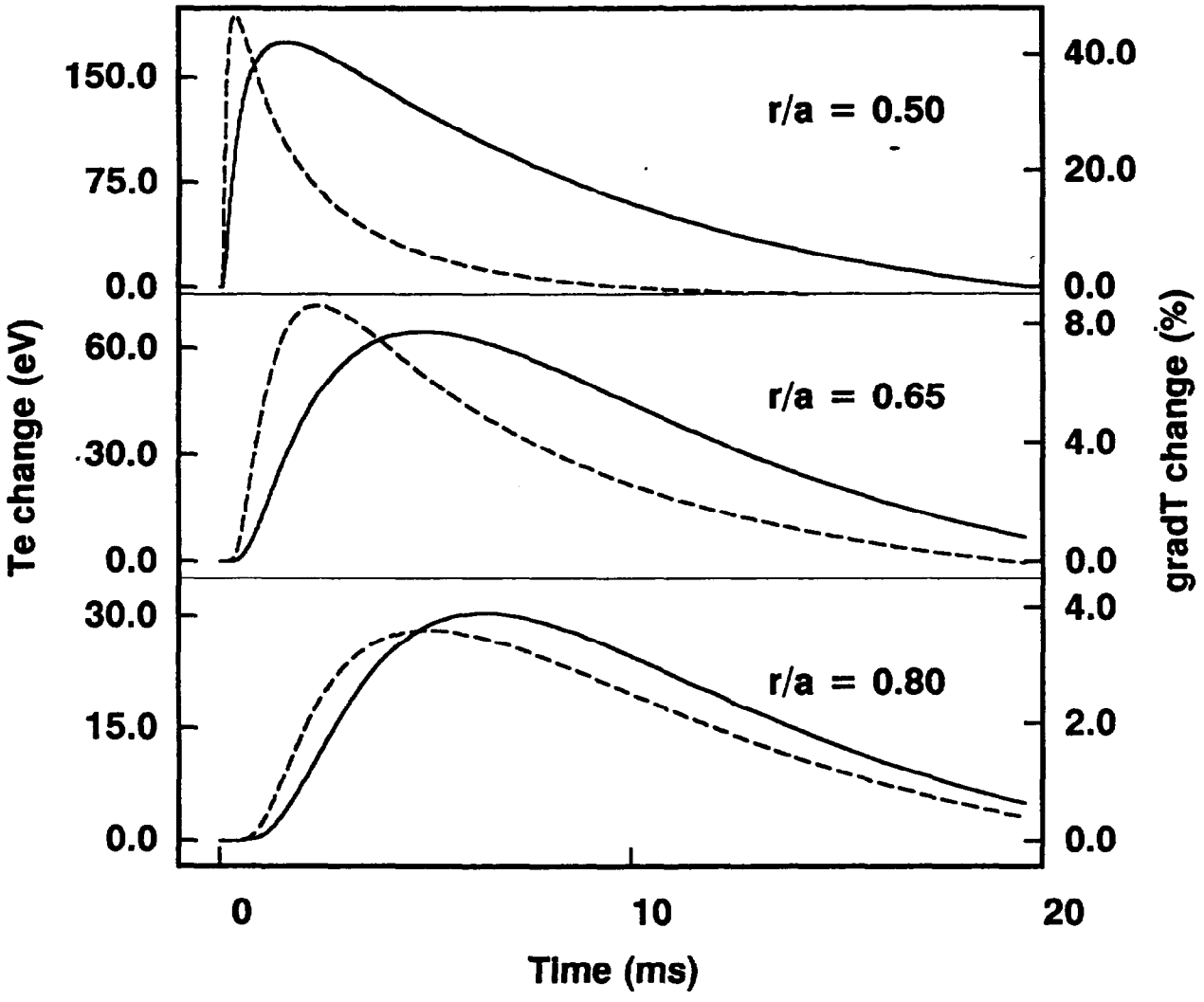

Figure 4

Since χ^{eff} is a function of ∇T, it varies during the heat pulse. Shown is the enhancement of ∇T (dashed line), which travels slightly ahead of the heat pulse (solid line).

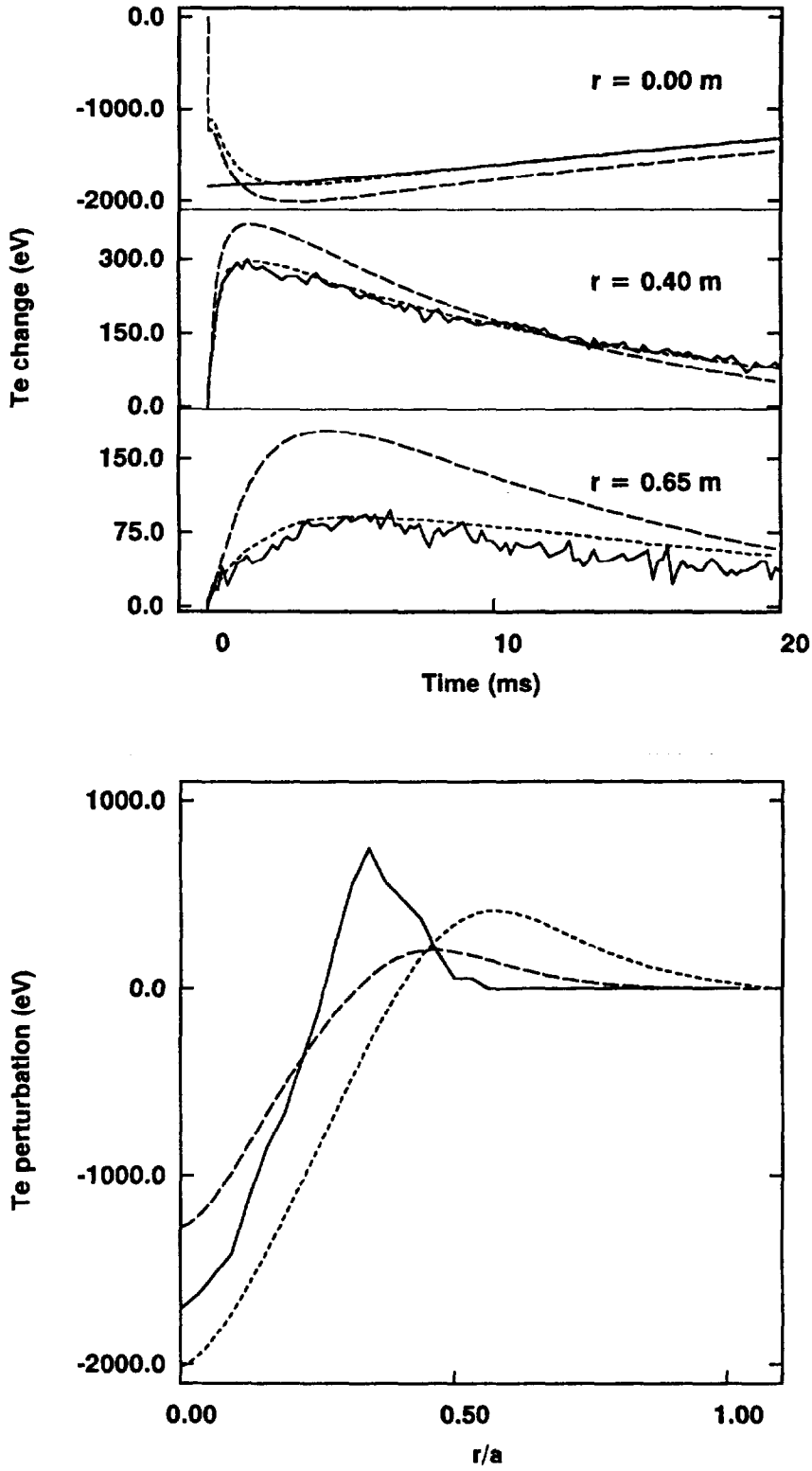

Figure 5

Results of modelling of the heat pulse using the same time dependent model and the measured T profiles as in [1]. a) Our results, using the TFTR model (dashed lines), compared with the published TFTR simulations [1] (dotted line). From this comparison it is apparent that the TFTR simulations are scaled by arbitrary factors to match the measurements. b) Simulations of electron temperature perturbation at 0.2 ms (dashed line) and 3 ms (dotted line), compared with the measured perturbation of the profile 0.2 ms after the sawtooth collapse (solid line).

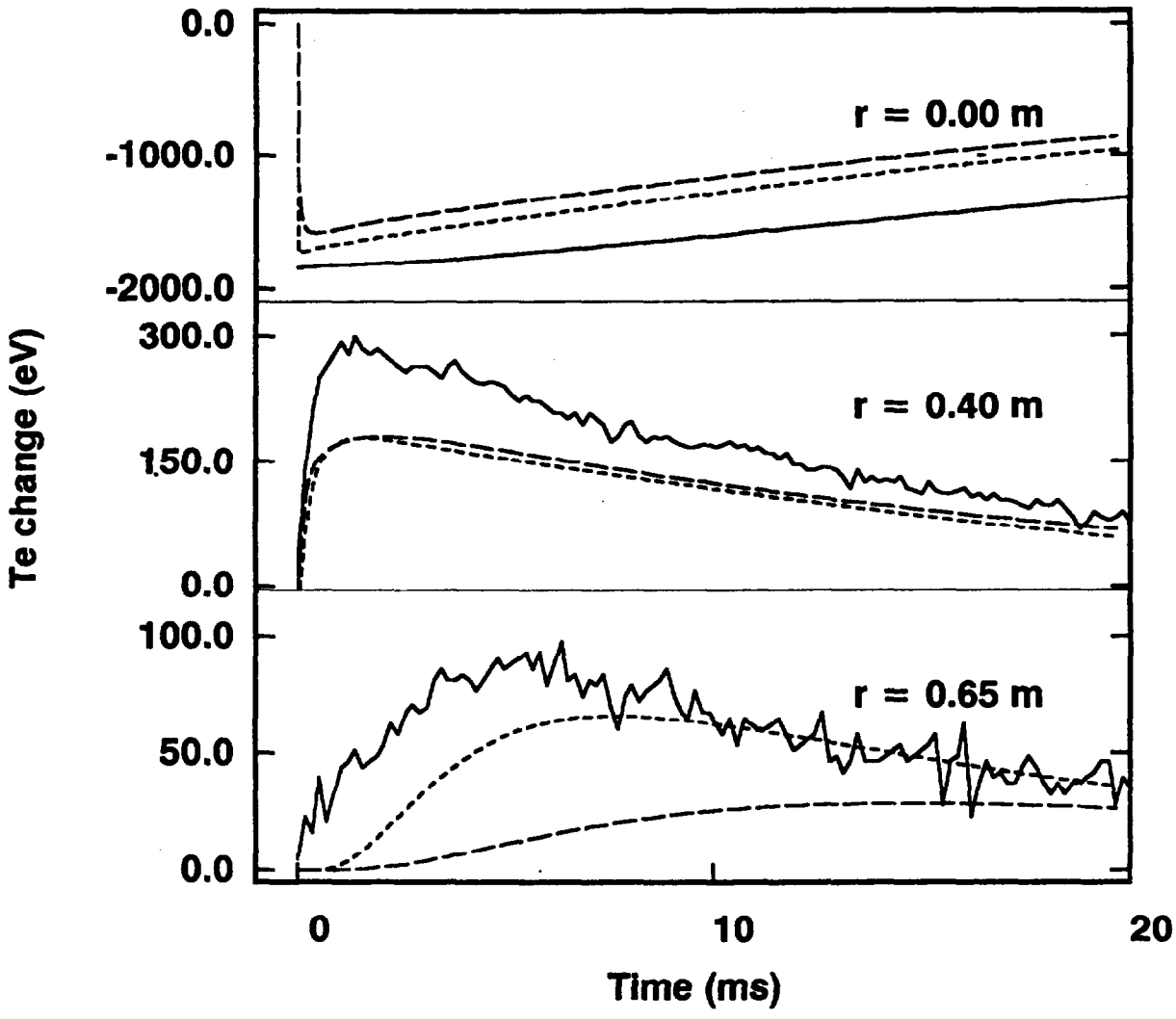

Figure 6

By reducing the time constant τ to 0.1 ms, a good fit to the data in the centre can be obtained, but the heat pulse is too slow (dashed lines). Even if the enhancement of χ^{eff} is limited to a region around r_{mix} it is not possible to match the data at all three radii (dotted lines).

APPENDIX 1.

THE JET TEAM

JET Joint Undertaking, Abingdon, Oxon, OX14 3EA, U.K.

J.M.Adams[1], F.Alladio[4], H.Altmann, R.J.Anderson, G.Appruzzese, W.Bailey, B.Balet, D.V.Bartlett, L.R.Baylor[24], K.Behringer, A.C.Bell, P.Bertoldi, E.Bertolini, V.Bhatnagar, R.J.Bickerton, A.Boileau[3], T.Bonicelli, S.J.Booth, G.Bosia, M.Botman, D.Boyd[31], H.Brelen, H.Brinkschulte, M.Brusati, T.Budd, M.Bures, T.Businaro[4], H.Buttgereit, D.Cacaut, C.Caldwell-Nichols, D.J.Campbell, P.Card, J.Carwardine, G.Celentano, P.Chabert[27], C.D.Challis, A.Cheetham, J.Christiansen, C.Christodoulopoulos, P.Chuilon, R.Claesen, S.Clement[30], J.P.Coad, P.Colestock[6], S.Conroy[13], M.Cooke, S.Cooper, J.G.Cordey, W.Core, S.Corti, A.E.Costley, G.Cottrell, M.Cox[7], P.Cripwell[13], F.Crisanti[4], D.Cross, H.de Blank[16], J.de Haas[16], L.de Kock, E.Deksnis, G.B.Denne, G.Deschamps, G.Devillars, K.J.Dietz, J.Dobbing, S.E.Dorling, P.G.Doyle, D.F.Düchs, H.Duquenoy, A.Edwards, J.Ehrenberg[14], T.Elevant[12], W.Engelhardt, S.K.Erents[7], L.G.Eriksonn[5], M.Evrard[2], H.Falter, D.Flory, M.Forrest[7], C.Froger, K.Fullard, M.Gadeberg[11], A.Galetsas, R.Galvao[8], A.Gibson, R.D.Gill, A.Gondhalekar, C.Gordon, G.Gorini, C.Gormezano, N.A.Gottardi, C.Gowers, B.J.Green, F.S.Griph, M.Gryzinski[26], R.Haange, G.Hammett[6], W.Han[9], C.J.Hancock, P.J.Harbour, N.C.Hawkes[7], P.Haynes[7], T.Hellsten, J.L.Hemmerich, R.Hemsworth, R.F.Herzog, K.Hirsch[14], J.Hoekzema, W.A.Houlberg[24], J.How, M.Huart, A.Hubbard, T.P.Hughes[32], M.Hugon, M.Huguet, J.Jacquinot, O.N.Jarvis, T.C.Jernigan[24], E.Joffrin, E.M.Jones, L.P.D.F.Jones, T.T.C.Jones, J.Källne, A.Kaye, B.E.Keen, M.Keilhacker, G.J.Kelly, A.Khare[15], S.Knowlton, A.Konstantellos, M.Kovanen[21], P.Kupschus, P.Lallia, J.R.Last, L.Lauro-Taroni, M.Laux[33], K.Lawson[7], E.Lazzaro, M.Lennholm, X.Litaudon, P.Lomas, M.Lorentz-Gottardi[2], C.Lowry, G.Magyar, D.Maisonnier, M.Malacarne, V.Marchese, P.Massmann, L.McCarthy[28], G.McCracken[7], P.Mendonca, P.Meriguet, P.Micozzi[4], S.F.Mills, P.Millward, S.L.Milora[24], A.Moissonnier, P.L.Mondino, D.Moreau[17], P.Morgan, H.Morsi[14], G.Murphy, M.F.Nave, M.Newman, L.Nickesson, P.Nielsen, P.Noll, W.Obert, D.O'Brien, J.O'Rourke, M.G.Pacco-Düchs, M.Pain, S.Papastergiou, D.Pasini[20], M.Paume[27], N.Peacock[7], D.Pearson[13], F.Pegoraro, M.Pick, S.Pitcher[7], J.Plancoulaine, J-P.Poffé, F.Porcelli, R.Prentice, T.Raimondi, J.Ramette[17], J.M.Rax[27], C.Raymond, P-H.Rebut, J.Removille, F.Rimini, D.Robinson[7], A.Rolfe, R.T.Ross, L.Rossi, G.Rupprecht[14], R.Rushton, P.Rutter, H.C.Sack, G.Sadler, N.Salmon[13], H.Salzmann[14], A.Santagiustina, D.Schissel[25], P.H.Schild, M.Schmid, G.Schmidt[6], R.L.Shaw, A.Sibley, R.Simonini, J.Sips[16], P.Smeulders, J.Snipes, S.Sommers, L.Sonnerup, K.Sonnenberg, M.Stamp, P.Stangeby[19], D.Start, C.A.Steed, D.Stork, P.E.Stott, T.E.Stringer, D.Stubberfield, T.Sugie[18], D.Summers, H.Summers[20], J.Taboda-Duarte[22], J.Tagle[30], H.Tamnen, A.Tanga, A.Taroni, C.Tebaldi[23], A.Tesini, P.R.Thomas, E.Thompson, K.Thomsen[11], P.Trevalion, M.Tschudin, B.Tubbing, K.Uchino[29], E.Usselmann, H.van der Beken, M.von Hellermann, T.Wade, C.Walker, B.A.Wallander, M.Walravens, K.Walter, D.Ward, M.L.Watkins, J.Wesson, D.H.Wheeler, J.Wilks, U.Willen[12], D.Wilson, T.Winkel, C.Woodward, M.Wykes, I.D.Young, L.Zannelli, M.Zarnstorff[6], D.Zasche[14], J.W.Zwart.

PERMANENT ADDRESS

1. UKAEA, Harwell, Oxon. UK.
2. EUR-EB Association, LPP-ERM/KMS, B-1040 Brussels, Belgium.
3. Institute National des Récherches Scientifique, Quebec, Canada.
4. ENEA-CENTRO Di Frascati, I-00044 Frascati, Roma, Italy.
5. Chalmers University of Technology, Göteborg, Sweden.
6. Princeton Plasma Physics Laboratory, New Jersey, USA.
7. UKAEA Culham Laboratory, Abingdon, Oxon. UK.
8. Plasma Physics Laboratory, Space Research Institute, Sao José dos Campos, Brazil.
9. Institute of Mathematics, University of Oxford, UK.
10. CRPP/EPFL, 21 Avenue des Bains, CH-1007 Lausanne, Switzerland.
11. Risø National Laboratory, DK-4000 Roskilde, Denmark.
12. Swedish Energy Research Commission, S-10072 Stockholm, Sweden.
13. Imperial College of Science and Technology, University of London, UK.
14. Max Planck Institut für Plasmaphysik, D-8046 Garching bei München, FRG.
15. Institute for Plasma Research, Gandhinagar Bhat Gujat, India.
16. FOM Instituut voor Plasmafysica, 3430 Be Nieuwegein, The Netherlands.
17. Commissiariat à L'Energie Atomique, F-92260 Fontenay-aux-Roses, France.
18. JAERI, Tokai Research Establishment, Tokai-Mura, Naka-Gun, Japan.
19. Institute for Aerospace Studies, University of Toronto, Downsview, Ontario, Canada.
20. University of Strathclyde, Glasgow, G4 ONG, U.K.
21. Nuclear Engineering Laboratory, Lapeenranta University, Finland.
22. JNICT, Lisboa, Portugal.
23. Department of Mathematics, Univeristy of Bologna, Italy.
24. Oak Ridge National Laboratory, Oak Ridge, Tenn., USA.
25. G.A. Technologies, San Diego, California, USA.
26. Institute for Nuclear Studies, Swierk, Poland.
27. Commissiariat à l'Energie Atomique, Cadarache, France.
28. School of Physical Sciences, Flinders University of South Australia, South Australia SO42.
29. Kyushi University, Kasagu Fukuoka, Japan.
30. Centro de Investigaciones Energeticas Medioambientales y Techalogicas, Spain.
31. University of Maryland, College Park, Maryland, USA.
32. University of Essex, Colchester, UK.
33. Akademie de Wissenschaften, Berlin, DDR.

CR 88.49.1A